Functionalization of Fluorinated Ionic Liquids: a Combined Experimental-Theoretical Study

Margarida L. Ferreira[a], João M. M. Araújo[a], Lourdes F. Vega[b], Fèlix Llovell[c], Ana B. Pereiro[a,*]

[a] LAQV, REQUIMTE, Departamento de Química, Faculdade de Ciências e Tecnologia, Universidade Nova de Lisboa, 2829-516 Caparica, Portugal. (mal.ferreira@campus.fct.unl.pt M.L.F.; anab@fct.unl.pt A.B.P.; jmmda@fct.unl.pt J.M.M.A.)

[b] Research and Innovation Center on CO_2 and H_2 (RICH), Center for Catalysis and Separation (CeCaS) and Chemical Engineering Department, Khalifa University, P.O. Box 127788, Abu Dhabi, United Arab Emirates. (lourdes.vega@ku.ac.ae L.F.V.)

[c] Department of Chemical Engineering and Materials Science, IQS School of Engineering, Universitat Ramon Llull, Via Augusta, 390, 08017, Barcelona, Spain. (felix.llovell@iqs.url.edu F.L.)

* Correspondence to: A.B. Pereiro, E-mail: anab@fct.unl.pt; Fax: (+351) 212948550; Tel: (+351) 212948318.

Abstract

We present new experimental and modeling data concerning imidazolium based-FILs synthesized with a hydroxyl group in the end of the cationic hydrogenated side chain and compared them with the analogous non-functionalized FILs in order to verify their suitability in the biomedical field. The thermophysical and thermodynamic properties of the neat coumpounds and the self-aggregation behavior of FILs in aqueous solutions were measured and compared with theoretical results from the soft-SAFT equation of state, in good agreement with each other. Results showed that the presence of the hydroxyl group increases the density and viscosity of pure compounds and aqueous mixtures, whereas the thermal stability, melting, free volume, ionicity and self-aggregation behavior decrease. These properties are improved with respect to the conventional perfluorosurfactants for the desired application, due to the full miscibility in water and the promising improved biocompatibility.

Keywords: Fluorosurfactants; hydroxyl group; thermophysical and thermodynamic properties; self-aggregation; soft-SAFT.

1. Introduction

The challenge of producing sustainable and green compounds has been one of the greatest efforts of academia and industries, prompting the development of "greener" ionic liquids (ILs). The major attribute of these compounds is the possibility to fine-tune their physicochemical properties by combining different cations and anions or functionalizing their structures, allowing the design of tailor-made ILs to specific applications [1,2].

The growing interest in task-specific ILs has empowered their functionalization through the introduction of functional groups in their structures, such as polar oxygenated features as hydroxyl, ester or ether groups [3]. The addition of polar groups can drastically reduce their cytotoxicity and ecotoxicity, as well as enhance their biodegradability, increasing their sustainability [4-7]. Several works showed that the introduction of a hydroxyl group in the cationic alkyl chain of imidazolium-based ILs decreases the thermal stability and self-aggregation behavior while increasing the viscosity, density, polarity and hydrophilicity [3,8-10].

Fluorinated Ionic Liquids (FILs) are a family of ILs with fluorinated tags equal or longer than four carbon atoms in either ions structures [11]. FILs can be designed with exceptional properties such as low surface tension, chemical and biological inertness, high surfactant power, low vapor pressures, and capacity to rearrange in stable self-assembled supramolecular systems [11,12]. The enhanced properties of FILs are a consequence of the formation of a fluorinated nanosegregated domain, leading to three distinct solvation regions (polar, hydrogenated and fluorinated domains), upgrading their solubilization power [13]. FILs are of great interest in areas where greener fluorinated compounds are required [14]. Then, the interest in FILs as potential biomaterials in life sciences and medicine has grown with the aim to be used as components of pharmaceuticals,

artificial oxygen carriers and biomolecules/drugs delivery systems [2,15]. These applications are related to their valuable characteristics, which make them enhanced nanomaterials: (i) FILs with short cationic hydrogenated chains showed a total miscibility in water; [16] (ii) they have improved surfactant power due to their amphiphilic behavior, allowing the formation of self-assembled aggregates in aqueous systems; [16,17] and (iii) they can have low acute ecotoxicity in aquatic organisms and negligible cytotoxicity in human cell lines [4,11,18].

The full characterization of FILs properties is a lengthy and expensive task and several theoretical approaches have arisen to enable a quick screening. One good example is the soft–Statistical Associating Fluid Theory (soft-SAFT) [19] which is a well-established Equation of State (EoS) grounded in statistical mechanical basis, where the intermolecular effects of a fluid are included in a coarse-grained molecular representation. In a recent work, [20] a thorough analysis of all FILs studied in literature by soft-SAFT proved its robustness to build FILs molecular models and accurately represent their structural features and properties in an intuitive way, keeping a high predictive capability [20].

In this work, two imidazolium-based FILs functionalized with a hydroxyl group in the tail of the cationic hydrogenated side chain (named as OH-FILs), conjugated with perfluorobutanesulfonate and perfluoropentanoate anions, were synthesized and characterized. (Table 1 shows structure and nomenclature). Melting and decomposition temperatures, density, viscosity, refractive index and conductivity were determined for OH-FILs. Moreover, the self-aggregation behavior, density, viscosity and ionic conductivity profile of OH-FILs in aqueous systems was analyzed. Previous work [4] shows that these OH-FILs have lower acute ecotoxicity than nonfunctionalized imidazoliums and pyridinium-based FILs. Results are discussed in terms of how the hydroxyl group can influence the pure and aqueous mixtures of FILs properties by comparing with the

analogous FILs without the hydroxyl group (see Table 1). Finally, the soft-SAFT EoS was used to build new molecular models for OH-FILs, describing the density and viscosity of the pure and binary systems with limited amount of experimental information. This theoretical approach allows us to better understand the microscopic behavior of OH-FILs, predicting the properties at different conditions and corroborating the experimental observations.

Table 1

Chemical structure and acronyms of the fluorinated ionic liquids cations and anions studied in this work.

Cations structure	Anions structure
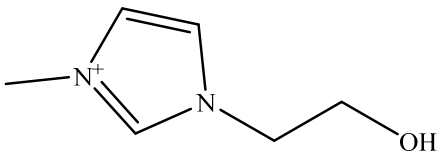	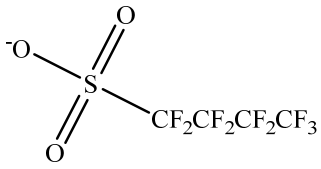
1-(2-hydroxyethyl)-3-methylimidazolium	Perfluorobutanesulfonate
$[C_{2(OH)}C_1Im]^+$	$[C_4F_9SO_3]^-$
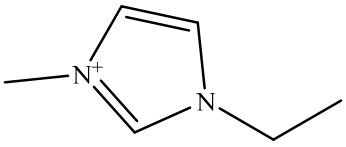	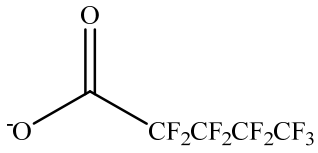
1-ethyl-3-methylimidazolium	Perfluoropentanoate
$[C_2C_1Im]^+$	$[C_4F_9CO_2]^-$

2. Soft-SAFT molecular models

Soft-SAFT EoS [19,21] is a variant of the well-established SAFT EoS [22,23] based on Wertheim's first-order thermodynamic perturbation theory for associating fluids [24-27]. Soft-SAFT accounts for the different molecular effects on a system as separated entities (*e.g.* molecular shape and association), enabling the description of the thermophysical properties and phase behavior of complex systems like ILs and their mixtures, in a good agreement with experimental data [28-33]. Further details on the equation can be found in Appendix A.

To accurately predict FILs properties through soft-SAFT EoS, a proper coarse-grained model has to be selected to describe the physical features of the FILs structure. This model is based on the assumption of the ILs intrinsic low ionic character due to the formation of short-lived ion pairs caused by the interactions between the ions, which are characterized through dispersion forces and specific steric interactions [34-36]. Through quantum information, molecular simulation results and previous experience, ILs are modelled as single chain molecules (cation and anion together) with a number of associating sites specified to account the highly anisotropic interactions between the counterions, such as hydrogen bonding [28-33]. Five molecular parameters must be defined to describe the molecules (chain length, m, spheres diameter, σ, and dispersive energy between monomers, ε) and the association scheme (site-site association energy, ε^{HB}, and volume, κ^{HB}).

A methodical study of all FILs parameterized by soft-SAFT EoS [20] underlined the robustness of this approach and disclosed a systematic procedure to modelling FILs. The parameterization is executed through the transference of the parameters between FILs with common cationic or anionic structures, simplifying the screening of similar compounds and their properties with less amount of experimental data [20]. The models of $[C_2C_1Im][C_4F_9SO_3]$ [28] and

[C_2C_1Im][$C_4F_9CO_2$] [29] were previously defined by three associating sites accounting for the counterions interactions and the negative charge delocatization caused by the fluorine and oxygen atoms. We had initially transferred this 3-association scheme to the model of [$C_{2(OH)}C_1Im$][$C_4F_9SO_3$] and [$C_{2(OH)}C_1Im$][$C_4F_9CO_2$]. However, the study of the electrostatic potential surfaces of OH-FILs (see Fig. 1), determined by using the MMFF94 force field [37] and performed through the open-source software Avogadro (version 1.2.0), [38] showed that this association scheme is not suitable. In fact, the addition of the hydroxyl group in the cationic hydrogenated chain contributes to higher charge delocalization and number of hydrogen bonding interactions between FILs cations. Consequently, a 5-site association scheme was selected: one associating site of type *A* represented the interactions between counterions, two sites of type *B* described the charge delocalization caused by the surrounding fluorines and the oxygens of the anion, and two additional sites were added to account for the hydroxyl group association, where a negative site *C* stands for oxygen and a positive site *D* for hydrogen (Fig. 1). To sum up, only interactions between *A*–*B*, *A*–*C*, *B*–*D* and *C*–*D* are allowed.

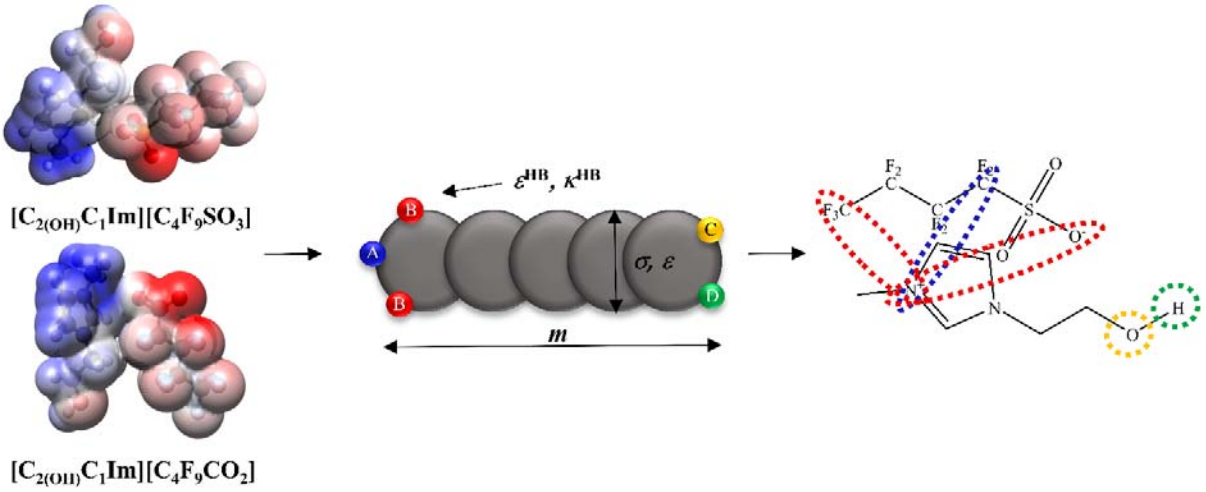

Fig. 1. Sketch of 5-associating sites model used to describe the hydroxyl-containing fluorinated ionic liquids within soft-SAFT framework. Blue and green represents the positive sites and red and yellow corresponds to negative sites.

To guarantee the definition of a suitable model based on the systematic methodology to parameterize FILs, [20] several molecular parameters of OH-FILs were transferred from the FILs-analogous values [28,29] following some restrictions [28-31,33] to reduce the parameters degeneracy and improve the transferability. As the anion is the structural feature that has higher influence in the transferability, [20] various parameters for FILs based on the same anion were transferred: the segments chain length, m, and the association parameters, ε^{HB} and κ^{HB}, were directly transferred from $[C_2C_1Im][C_4F_9SO_3]$ [28] and $[C_2C_1Im][C_4F_9CO_2]$, [29] to $[C_{2(OH)}C_1Im][C_4F_9SO_3]$ and $[C_{2(OH)}C_1Im][C_4F_9CO_2]$, respectively. For the two additional associating sites added to represent the interactions of the OH–OH groups, the association strength was transferred from ethanol model (ε^{HB}/k_B=2388 K and κ^{HB}=2932 Å^3). [39] Besides, cross-association between OH group and the anion/cation counterparts are allowed (*A–C*, *B–D* interactions). Then, the association strength values were calculated using the combining rules given in Eqs. A.4 and A.5 in Supplementary Data. The remaining segment diameter, σ, and

dispersive energy between segments, ε, for both OH-FILs were obtained by fitting to the experimental density data at atmospheric pressure. The final parameters sets of OH-FILs can be found in Table 2, as well as those previously published for the analogous FILs [28,29]. The binary mixtures of FILs + water were also studied, details on water model are in Appendix A, with soft-SAFT parameters provided in Table 2 [40]. Cross-association interactions between FILs and water molecules were calculated using combining rules (Eqs. A.4 and A.5 in Supplementary Data).

Table 2

Molecular weight, molecular parameters and absolute average deviation (AAD) for the densities of the studied fluorinated ionic liquids and water.

Substance	M_w [g·mol^{-1}]	m	σ [Å]	ε/k_B [K]	ε^{HB}/k_B [K]	κ^{HB} [Å^3]	AAD [%]
$[C_{2(OH)}C_1Im][C_4F_9SO_3]$	426.26	7.320	3.818	324.0	3850	2250	0.028
$[C_{2(OH)}C_1Im][C_4F_9CO_2]$	390.21	7.233	3.788	328.1	3850	2250	0.046
$[C_2C_1Im][C_4F_9SO_3]$[a]	410.26	7.320	3.816	343.4	3850	2250	0.053
$[C_2C_1Im][C_4F_9CO_2]$[b]	374.21	7.233	3.762	338.8	3850	2250	0.008
Water[c]	18.01	1.000	3.154	365	2388	2932	

Parameters from references [28] for (a); [29] for (b) and [40] for (c).

3. Results and discussion

$[C_{2(OH)}C_1Im][C_4F_9SO_3]$ and $[C_{2(OH)}C_1Im][C_4F_9CO_2]$ FILs were synthesized pursuing the functionalization of the analogous FILs, $[C_2C_1Im][C_4F_9SO_3]$ and $[C_2C_1Im][C_4F_9CO_2]$ [12]. The melting point, thermal stability, density, viscosity, refractive index, ionic conductivity, and the

calculated fluidity and free volume parameters were studied to experimentally characterize them. The self-aggregation behavior of OH-FILs in aqueous solutions was obtained by measuring the density and viscosity as well as determining the critical aggregation concentrations (CACs) and the ionization degree of the aggregates. Moreover, the density and viscosity of the pure OH-FILs and of the FILs + water systems were characterized with soft-SAFT EoS to better understand the microscopic behavior of OH-FILs and to corroborate the experimental observations. This study discloses the influence on the physicochemical properties caused by the addition of a hydroxyl group in FILs, since it increases the biocompatibility and enhances their properties to be used in biological applications [4-7]. Consequently, the discussion is focused on two different structural features: (i) the influence induced by introducing a hydroxyl group in the cation structure and (ii) the influence of the anions $[C_4F_9SO_3]^-$ and $[C_4F_9CO_2]^-$ in these properties.

3.1. Thermal analysis

Thermal properties are crucial to decide the eligibility of a substance to a specific application, because the melting and decomposition temperatures determine the liquid and operative range of FILs. Thus, the onset temperature, T_{onset}, starting temperature, T_{start}, melting temperature, T_m, and glass transition temperature, T_g, for OH-FILs were measured (Table A.1 in Supplementary Data). In Fig. 2, the T_{onset} versus T_m results were compared with the analogous FILs values previously reported [12]. In order to consider their applicability in biomedical applications, thermal stability must be ensured under 310.15 K (the human body temperature, black line in Fig. 2). FILs with T_m above this value are discarded, preferring those with higher T_{onset} values. All FILs showed a value of T_m lower than 310.15 K, and regarding the influence of the hydroxyl group, OH-FIL conjugated with $[C_4F_9SO_3]^-$ anion has lower T_m and T_{onset} values than with the $[C_2C_1Im]^+$ cation. The opposite behavior was observed for $[C_4F_9CO_2]^-$ anion, where $[C_{2(OH)}C_1Im]^+$ cation has higher values of T_m

and T_{onset}. The anion influence shows that $[C_4F_9SO_3]$-FILs have higher values of T_{onset}. However, T_m is higher for OH-FIL based on $[C_4F_9CO_2]^-$ anion. It can be inferred that both structural features (hydroxyl group and anion) highly influence these thermal properties. Nonetheless, all FILs show an adequate thermal behavior and the best T range was observed for $[C_{2(OH)}C_1Im][C_4F_9SO_3]$ due to the combination of a low T_m and a high T_{onset}. All FILs have T_m under 298.15K, ensuring thermal stability at room temperature, regarding the compound's handling and storage. Another interesting feature is that both OH-FILs have a T_g (Table A.1 in Supplementary Data), whereas the analogous FILs did not show any T_g in the studied temperature range [12].

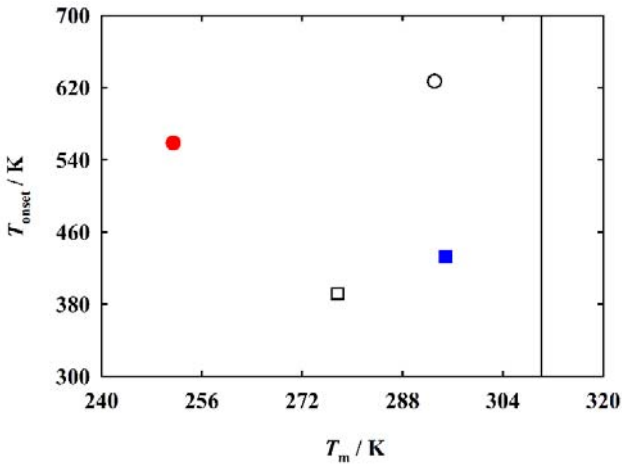

Fig. 2. Decomposition onset temperature versus melting temperature for $[C_{2(OH)}C_1Im][C_4F_9SO_3]$ (red, ●) and $[C_{2(OH)}C_1Im][C_4F_9CO_2]$ (blue, ■) FILs and comparison with $[C_2C_1Im][C_4F_9SO_3]$ (black, ○) and $[C_2C_1Im][C_4F_9CO_2]$ (black, □) literature values [12]. The line indicates the reference temperature of human body, 310.15 K.

3.2. Thermophysical and transport properties

FILs are tunable compounds and any alteration in their structure allows changes their thermophysical and transport properties. [41,42] Then, density, viscosity and conductivity have

been analysed. In addition, refractive index, related to the molar free-volume effects, forces between ILs molecules and their behavior in solution, [43] are also relevant for assessing their application.

3.2.1. Density and viscosity

The density and viscosity of OH-FILs were measured (Table A.2 in Supplementary Data) and the results are illustrated in Fig. 3. The values previously determined for analogous FILs are also represented for comparative purposes [12]. Fig. 3a shows the density results, where all FILs values linearly decrease when the temperature increases. The same behavior was found for other FILs in earlier publications [12,44]. The comparison between $[C_{2(OH)}C_1Im]$- and $[C_2C_1Im]$-FILs shows that the hydroxyl group significantly increases the density of the FILs. Besides, the $[C_4F_9SO_3]$-FILs present higher densities than those with the $[C_4F_9CO_2]^-$ anion. Finally, $[C_2C_1Im][C_4F_9CO_2]$ ($1.47 g \cdot cm^{-3}$ at 313.15 K) is the FIL with lower density.

The provided experimental data were used to parameterize the OH-FILs using soft-SAFT EoS, as explained in "soft-SAFT molecular models" Section. The resulting model calculations are plotted as solid lines in Fig. 3a, showing an excellent agreement with experimental data (deviations lower than 0.05%). Soft-SAFT calculations related to the analogous FILs [28,29] are plotted as dashed lines in Fig. 3a.

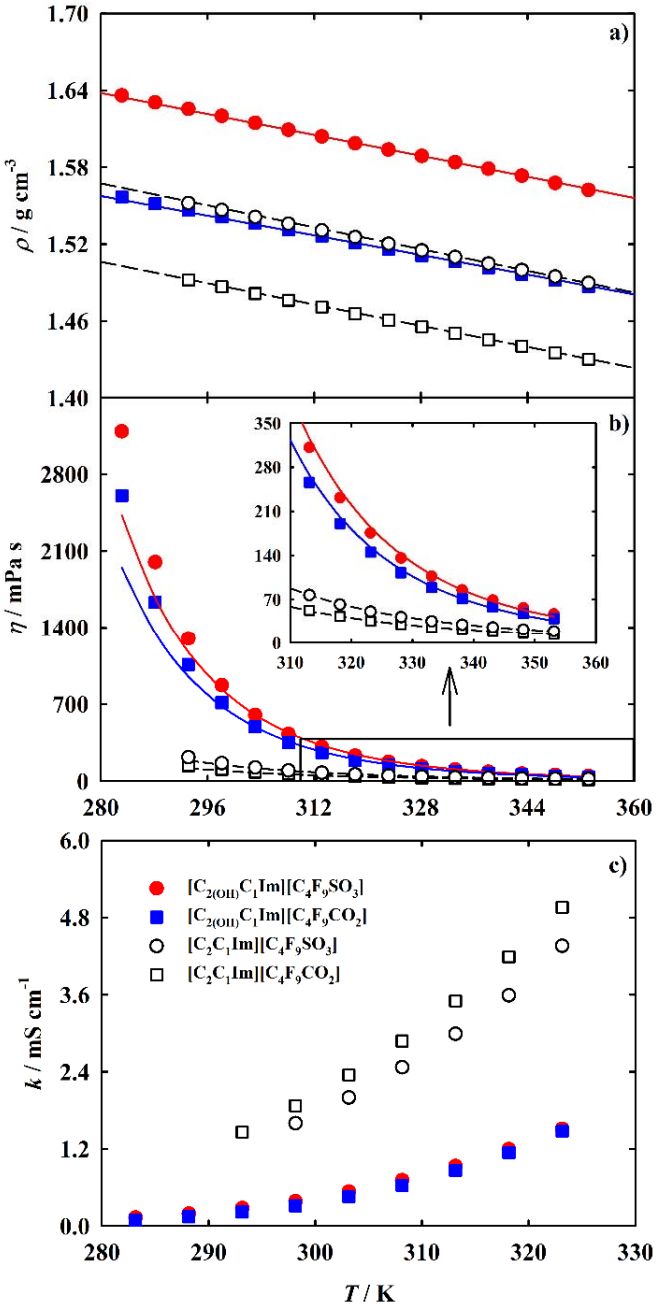

Fig. 3. Density (a), dynamic viscosity (b) and ionic conductivity (c) versus temperature at atmospheric pressure, for the pure FILs studied in this work, ($[C_{2(OH)}C_1Im][C_4F_9SO_3]$ and $[C_{2(OH)}C_1Im][C_4F_9CO_2]$), and for the analogous FILs, [12] ($[C_2C_1Im][C_4F_9SO_3]$ and $[C_2C_1Im][C_4F_9CO_2]$). The lines in (a) and (b) represent the soft-SAFT calculations (solid lines for OH-FILs and dashed lines for analogous FILs).

In order to verify the consistency and physical meaning of the fitted molecular parameters of the OH-FILs, two correlations of the molecular parameters with the molecular weight (M_w) of FILs were used (Fig. A.1 in Supplementary Data). The $m\sigma^3$ refers to a rough approximation of the volume of the ILs individual molecules (volume of each group multiplied by the chain length), while $m\varepsilon$ refers to the energy of the ILs molecules. The $m\sigma^3$ values (Fig. A.1a in Supplementary Data) of [$C_4F_9CO_2$]-FILs have a proportional increment with the M_w, whereas the [$C_4F_9SO_3$]-FILs do not show significant differences. Since the m parameter was transferred from FILs [28,29] to OH-FILs, the volume differences from the addition of the hydroxyl group are considered by the σ parameter (Fig. A.1a in Supplementary Data). The OH-FILs show a higher M_w and a lower $m\varepsilon$ value compared to the analogous FILs,[28,29] indicating that the addition of the OH group minimizes the inner van der Waals energy of the FILs molecules (Fig. A.1b in Supplementary Data).

In Fig. 3b the viscosity data of OH-FILs and the analogous FILs is plotted [12]. The analysis of these results shows a high dependence and inverse proportionality with temperature. The addition of the hydroxyl group severely increases the viscosity, which can be related to the increment of the cationic interactions.[8] Conversely, the viscosity is higher for [$C_4F_9SO_3$]-FILs than for [$C_4F_9CO_2$]-FILs.

In order to gain molecular insights into the behavior of the systems, the viscosity data was theoretically characterized by soft-SAFT coupled with FVT, [45,46] as described in Section 2.2. of Appendix A. Results are depicted in Fig. 3b where a good agreement with experimental values is observed. Only a small deviation between the two experimental points at the lowest temperatures are found. The FVT parameters are given in Table A.3 (Supplementary Data).

Results of viscosity and density show that OH-FILs and [$C_4F_9SO_3$]-FILs present higher cohesive structures, resulting in more dense and viscous compounds. As expected, higher fluidity is found for non-functionalized FILs with the $[C_4F_9CO_2]^-$ anion.

3.2.2. Molar free-volume effects

Refractive index enables the measurement of the electric polarizability of a molecule, providing useful information about the response of the molecules electron distribution to an electric field, which can also be induced by electric interactions with ionic solvents, allowing the study of the internal structure of molecules and their bounded systems [43,47]. Data for OH-FILs regarding the refractive index are presented in Table A.2 (Supplementary Data), showing inverse proportionality with temperature, the same behaviour of the analogous FILs [12]. The results indicate slightly higher values for $[C_{2(OH)}C_1Im][C_4F_9CO_2]$ in comparison with the other FILs.

Considering the importance of defining the ability of FILs to dissolve, the molar free-volume effects was calculated for OH-FILs by Lorentz-Lorentz equation [47] (more details can be found in Appendix A). The calculated values of the molar refractions and molar volumes of OH-FILs are listed in Table A.4 (Supplementary Data) and they were also compared with the ones from analogous FILs [12]. The analysis of the molar refractions showed the tendency $[C_2C_1Im][C_4F_9CO_2] < [C_{2(OH)}C_1Im][C_4F_9CO_2] < [C_{2(OH)}C_1Im][C_4F_9SO_3] < [C_2C_1Im][C_4F_9SO_3]$; whereas the molar volumes are $[C_2C_1Im][C_4F_9CO_2] \approx [C_{2(OH)}C_1Im][C_4F_9CO_2] < [C_{2(OH)}C_1Im][C_4F_9SO_3] \approx [C_2C_1Im][C_4F_9SO_3]$. The relative ratio of the free volume over molar volume, $f_m V_m^{-1}$, was also calculated in this work [12,28,44] (see the methodology in Appendix A along with the values in Table A.4). The analysis of $f_m V_m^{-1}$ indicated that the effect of the anion and of the addition of a hydroxyl group is not significant (with slightly lower ratio values for

[$C_{2(OH)}C_1Im$][$C_4F_9CO_2$]). The increment of the cationic interactions due to the OH group can compact the structure of the OH-FIL, diminishing the free spaces caused by the asymmetric counterions and bulky imidazolium cation of the analogous compounds.

3.2.3. Walden plot

The ionic conductivities of OH-FILs are reported in Fig. 3c and Table A.2 (Supplementary Data). The results show no significant differences between OH-FILs. The addition of the hydroxyl group decreases the ionic conductivity of OH-FILs, which can be related with the decrement of fluidity associated to the polar interactions by cationic OH groups, compacting the structure of the OH-FILs, diminishing their mobility. Fig. 4 reports the ionicity of the OH-FILs studied and the analogous FILs [12]. This property establishes a relation between the molar conductivity and the fluidity (inverse of viscosity) of a solution using the Walden Plot (Fig. 4). Ionicity provides useful information about transport properties, mobility and the possible formation of aggregates, whose presence decreases the mobility of FILs and increases their viscosity, resulting in an ionic behaviour away from the ideal electrolyte [11,12]. The ionicity of these compounds is mainly controlled by the molar concentration of ions, the charged aggregates and their mobility in the fluid. Thus, this property is a measure of the formation of aggregates due to the decrease of fluidity and conductivity of a compound. The standard classification of ionic liquids using the Walden plot (Fig. 4a) is pictured by a straight line representing the ideal behaviour corresponding to aqueous KCl solutions (fully dissociated, where the ions have equal mobility). In Fig. 4b, a closer look into the Walden plot shows a linear trend with temperature observed for each pure FIL. The ionicity is very similar for all FILs, with slightly higher values for [$C_4F_9SO_3$]-FILs. The hydroxyl group functionalization does not affect this property.

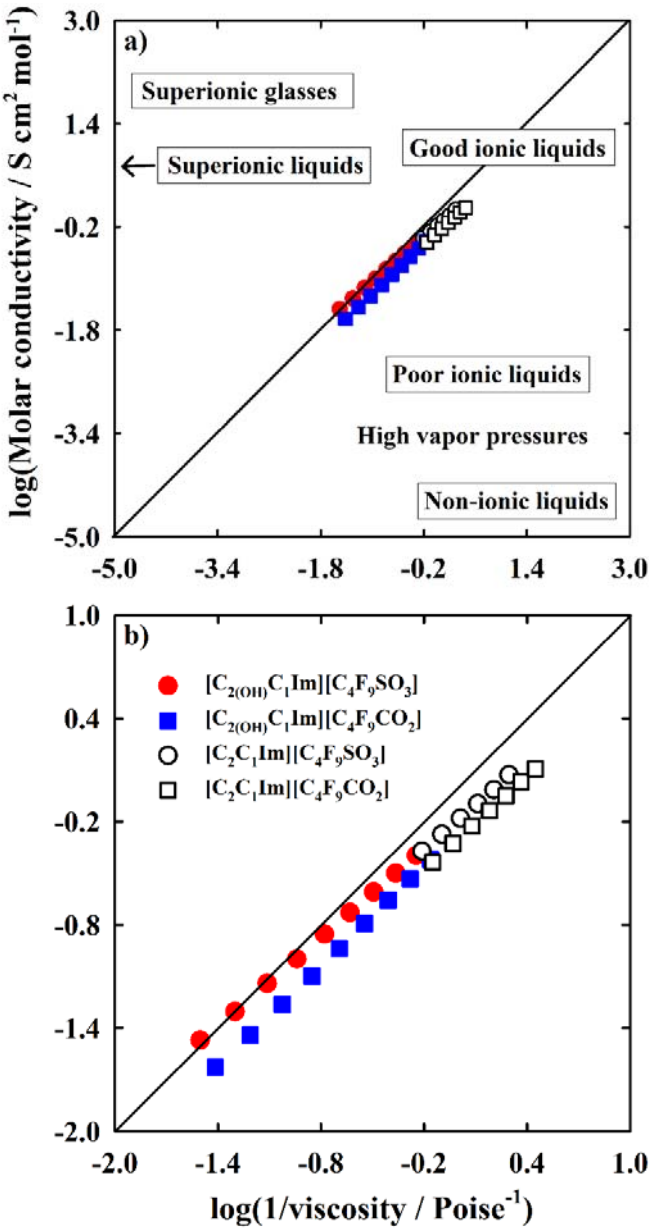

Fig. 4. (a) Classification diagram for ionic liquids based on the Walden plot and (b) a closer look for the pure FILs studied in this work, ($[C_{2(OH)}C_1Im][C_4F_9SO_3]$ and $[C_{2(OH)}C_1Im][C_4F_9CO_2]$), in a temperature range of 283.15-323.15 K and for the analogous FILs, [12] ($[C_2C_1Im][C_4F_9SO_3]$ and $[C_2C_1Im][C_4F_9CO_2]$).

3.3. Self-aggregation behaviour of fluorinated ionic liquids in aqueous solutions

Knowledge on the self-aggregation behaviour and solvation mechanisms of FILs and how the structural features can affect the organization of the self-assembled components will allow the design of new compounds with improved surfactant power. In this section, the density, viscosity, ionicity and the critical aggregation concentrations (CACs) of FILs + water systems are disclosed. These results elucidate the insight of the OH-FILs self-aggregation mechanism in water and the verification of their usefulness as totally water-miscible fluorinated surfactants.

3.3.1. Density, viscosity and ionicity

The density and viscosity of the $[C_{2(OH)}C_1Im][C_4F_9SO_3]$, $[C_{2(OH)}C_1Im][C_4F_9CO_2]$ and $[C_2C_1Im][C_4F_9CO_2]$ FILs in aqueous solutions were determined in this work between 298.15 and 318.15 K, whereas the ionic conductivity of OH-FILs was determined at 298.15 K (Table A.5 in Supplementary Data). The results were compared with the previous measurements of $[C_2C_1Im][C_4F_9SO_3]$ + water system [16]. The density and viscosity at 298.15 K are represented in Fig. 5, (the other temperatures are plotted in Figs. A.2 and A.3 in Supplementary Data, respectively). As expected, the increment of temperature decreases the density and viscosity of the binary systems. Through the detailed analysis of Fig. 5, the increment of water concentration reduces both properties. The results show the same trends obtained for the pure components, where higher values of density and viscosity are found to OH-FILs and $[C_4F_9SO_3]$-FILs.

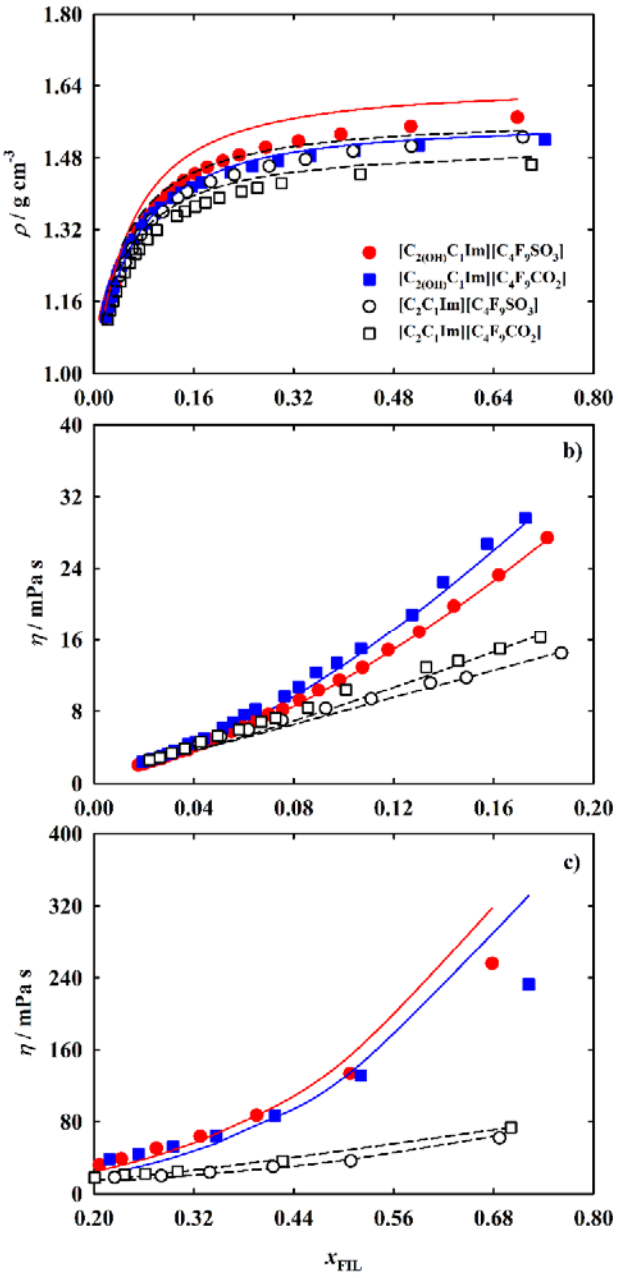

Fig. 5. Density (a) and dynamic viscosity for the x_{FIL} range between 0 to 0.2 (b) and for the x_{FIL} range between 0.2 to 0.8 (c) versus FILs composition for the $[C_{2(OH)}C_1Im][C_4F_9SO_3]$, $[C_{2(OH)}C_1Im][C_4F_9CO_2]$ and $[C_2C_1Im][C_4F_9CO_2]$ determined in this work at 298.15 K, and for $[C_2C_1Im][C_4F_9SO_3]$ [16]. The lines represent the soft-SAFT + FVT calculations (solid lines for OH-FILs and dashed lines for analogous FILs).

In Fig. 5a, the predicted density by soft-SAFT EoS (lines) shows a good agreement with experimental data, although the density is slightly overestimated in the concentration range 0.2-1.0 molar fraction of FIL (x_{FIL}). Though, the qualitative trend is well represented. It is important to stress out that no fitting to the binary data were used, being the results a full prediction from the parameters adjusted to the pure FILs data. This empowers the modelling approach to predict other mixture conditions for which not experimental data are available. The calculations related to all range of temperatures are represented by the solid lines in Figs. A.2 and A.3 (Supplementary Data).

Two approaches were executed in the viscosity description of the FILs + water system using soft-SAFT + FVT [45,46]. Firstly, the Spider-Web methodology [48] (see Section 2.2. of Appendix A) was used to reproduce the viscosity in all FILs composition range. However, the calculations did not show good agreement with the experimental data, as depicted in Fig. A.4 (Supplementary Data), where the calculations for all FILs at 298.15 K are represented as an example. Looking at the tendency of the experimental data and the change of behaviour in the viscosity before and after a concentration of 0.2, x_{FIL} a second approach was used. The Spider-Web methodology was applied to optimize two sets of FVT parameters characterizing the ranges of 0-0.2 (Fig. 5b) and 0.2-0.8 (Fig. 5c) of x_{FIL} (see FVT parameters on Table A.3 in Supplementary Data). As a consequence, different values of L_v and B were obtained while the α parameter was the same for the whole range of composition for each FIL. The use of two different sets of parameters is not usually executed in the soft-SAFT + FVT approach, but it has been previously used for describing the VLE of water, [40] to take into account the anomalous behaviour of the density at low temperatures. In this case a similar procedure has been considered for the FTV part, as the nanosegregation (applicable to higher concentrations and pure FIL) [13] and the different structuration behaviour of the molecules in aqueous solutions (evident in the range of lower FIL

compositions) [16,17] has a direct impact in the viscosity of the fluid. These structural changes cannot be considered neither by soft-SAFT theory nor by Free-Volume Theory approach, which are mean-field theories. Moreover, the very sharp decrease of the viscosity of the FILs after the addition of a few amount of water, which is associated with the mentioned structural changes, also difficult the viscosity modelling of water + FILs systems. This highly non-ideal behaviour can hardly be captured by the FVT method, for the reasons already mentioned; more detailed molecular approaches, such as molecular simulations should be used, but they are out of the scope of the current work. As far as the predictive power of the equation is concerned, It is also important to mention that the extension of the soft-SAFT FVT calculation to mixtures was done without the addition of any binary parameters for the viscosity. A change in the mixing rules, allowing the use of fitting binary parameters, can help to improve the description of aqueous systems [49] but this solution is more related to a less constrained model (with extra parameters) than including a physical interpretation of the behaviour of the mixture.

The ionicity of FILs + water systems was obtained in the same way as for the pure systems (see "Walden plot" Section) and represented in Fig. 6. Experimental data for OH-FILs + water ionic conductivity were determined (Table A.5 in Supplementary Data) and compared with the former $[C_2C_1Im][C_4F_9SO_3]$ + water system [16]. The experimental results show that all the three systems have a similar ionicity behaviour (similar vertical distance to the ideal electrolyte line along of each own profile) (Fig. 6). Interestingly, an increment of ionicity from pure FIL until a maximum at a certain x_{FIL} value is observed. After this value, the ionicity starts to decrease when the x_{FIL} decreases. This behaviour is more evident to the $[C_4F_9SO_3]$-FILs. The maximum can be related to the extremely high ionic conductivity that will be scrutinized in the next section. The addition of the hydroxyl group (comparing $[C_{2(OH)}C_1Im][C_4F_9SO_3]$ and $[C_2C_1Im][C_4F_9SO_3]$) decreases the

"ideal" behaviour (more distance to the ideal electrolyte line) in the region of higher x_{FIL} and increases it in the lower x_{FIL}. Comparing both OH-FILs, the $[C_4F_9SO_3]^-$ anion shows values closer to the "ideal" electrolyte than $[C_4F_9CO_2]^-$. These results indicate the formation of distinct aggregates of FILs in the aqueous solutions. These outcomes will be further supported by the analysis of the complete conductivity profile and CACs of OH-FILs in the next section.

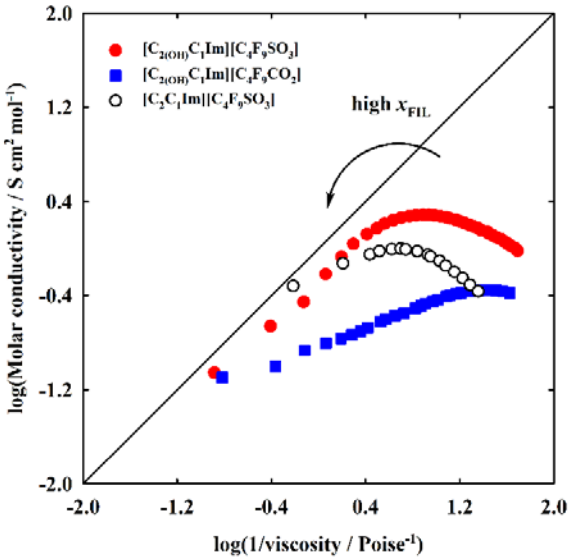

Fig. 6. Walden plot of $[C_{2(OH)}C_1Im][C_4F_9SO_3]$ + water and $[C_{2(OH)}C_1Im][C_4F_9CO_2]$ + water binary systems at 298.15 K. For comparison purposes, the Walden plot of $[C_2C_1Im][C_4F_9SO_3]$ + water system was also included [16]. The arrow indicates the increment of molar fraction of the FILs in solution.

3.3.1. Critical aggregation concentrations

Amphiphilic molecules aggregate in aqueous solutions depending on the species and the medium. The formation of orientated colloidal aggregates occurs when the concentration of those species with long hydrophobic chains surpasses certain value. This leads to variation in the physicochemical properties and the narrow ranges of concentrations are known as CACs. According to Philips et al., [50] the first CAC, known as critical micellar concentration (CMC), corresponds to the value of concentration in which a first maximum change in gradient appears

when plotting ionic conductivity versus concentration. In this context, measurements of ionic conductivity are usually implemented in the ionic micellar studies [16,17,51]. The ionic conductivity of FIL aqueous solutions was measured at 298.15 K for OH-FILs (Fig. 7a) and compared with the analogous FILs [16,17]. The ionic conductivity data against x_{FIL} are illustrated in Fig. 7a, where full miscibility in water is observed for the complete range of concentration (from pure water to pure FIL) of OH-FILs. Following Philips' definition, [50] already implemented in FILs, [16,17,51] the CACs were determined, and values are reported in Table 3. The analysis of Fig. 7a shows that the gradual addition of FIL to water presents similar tendencies as in the literature, exhibiting two phases: a first step in which the ionic conductivity increases, followed by a second step in which values decrease after reaching a maximum [16]. This is the same behaviour found for the Walden Plots previously discussed. The mentioned increase in ionic conductivity in diluted systems can be explained by the rising number of free ions in the solution. However, at the CAC value, the number and mobility of charge carriers is reduced due to the increase in aggregate formation and the decrease in fluidity, resulting in a deviation from the linear behaviour [16].

Although all the studied FILs have multiple CACs, the most significant change in ionic conductivity behaviour occurs at lower values of x_{FIL}, corresponding to the CMC (Table 3). Two more transitions were determined at lower x_{FIL}, corresponding to second and third CACs (Table 3). The changes in the slopes of these plots were analysed according to Phillips definition, [50] and compared with the bibliographic values of $[C_2C_1Im][C_4F_9SO_3]$ [16] and $[C_2C_1Im][C_4F_9CO_2]$ [17] (Fig. 7b and Table 3). The three CACs can be related to the FILs total miscibility in water, indicating the formation of different structures along the increment of x_{FIL}, concluding that a low x_{FIL} is enough to assemble into colloidal aggregates. From the analysis of the influence of the FILs

structural features in the CACs, it is shown in Fig. 7b that the addition of a hydroxyl group: (i) does not significantly affect the CMC values; (ii) increases the second CAC on the case of $[C_4F_9SO_3]$-FILs while does not significantly affect that of the $[C_4F_9CO_2]$-FILs; and (iii) increases the third CAC of $[C_4F_9SO_3]$-FILs and decreases the value of $[C_4F_9CO_2]$-FILs. The $[C_2C_1Im][C_4F_9SO_3]$ shows the best self-aggregation behaviour, with lower values for all three CACs. All FILs studied, with only 4 carbon atoms in the anionic fluorinated tags, have an improved surfactant behaviour compared to the CMC values of the conventional perfluorosurfactants and their hydrogenated counterparts, with fluorine tags of 8 carbons (approximately 30 $mmol.kg^{-1}$ for sodium perfluorooctanoate and ammonium perfluorooctanoate and 380 $mmol.kg^{-1}$ for sodium octanoate) [52-54].

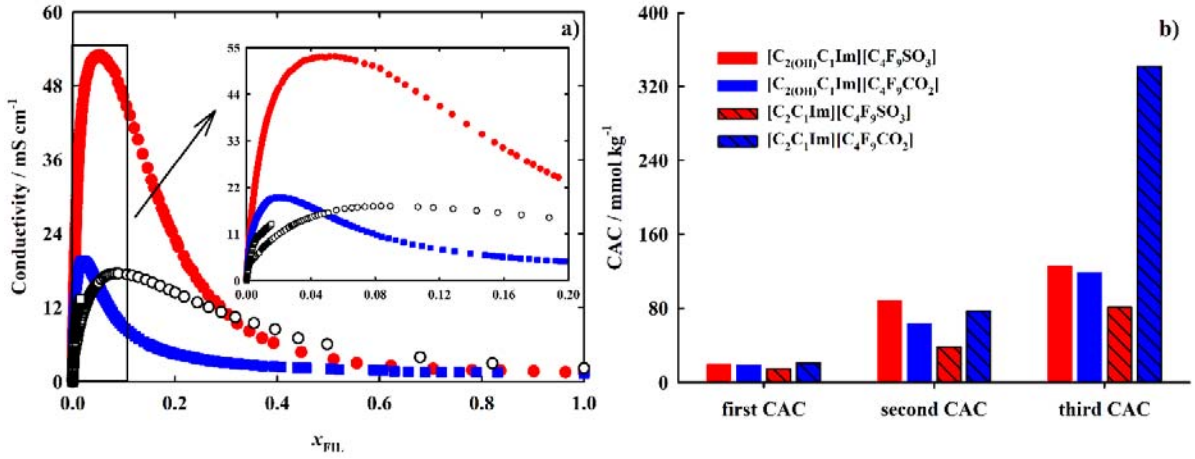

Fig. 7. (a) Conductivity profile of $[C_{2(OH)}C_1Im][C_4F_9SO_3]$ (red, ●) and $[C_{2(OH)}C_1Im][C_4F_9CO_2]$ (blue, ■) in aqueous solution at 298.15 K, determined in this work, and for $[C_2C_1Im][C_4F_9SO_3]$ (black, ○) and $[C_2C_1Im][C_4F_9CO_2]$ (black, □) [16,17]. (b) Critical aggregation concentration (CAC) values of OH-FILs in aqueous solution at 298.15 K determined in this work and for analogous FILs [16,17].

The degree of ionization of the aggregates, represented by α, can be found in Table 3. This parameter is associated to the charges fraction of the surfactant ions in the micelles, which suffer

neutralization through the micelle-bound counterions. It is calculated by the ratio of the linear segments slopes above and below the CACs. Even if the surfactant ions are supposedly dissociated in aqueous solutions, the molecules are partly associated with the counterions, enabling the formation of aggregates [16,17]. Therefore, a lower α value means an improved micelle packaging. Furthermore, the degree of counterion binding/condensed on the micellar surface was also determined, which derives from the degree of ionization as follows:

$$\beta = 1 - \alpha \quad [1]$$

This β parameter can be correlated with the charge density at the aggregate surface, the aggregate size, and the hydrophobic nature of the counterions [16,17]. The increment of α values, and consequently decrease of β values, in the first and third transitions (Table 3, comparison between $[C_{2(OH)}C_1Im][C_4F_9SO_3]$ and $[C_2C_1Im][C_4F_9SO_3]$ [16]) proves that the aggregates can lose the packaging in their structures because OH group increases the FILs polarity. The second transition does not have significant changes. This variation is observed in second and third transitions for $[C_{2(OH)}C_1Im][C_4F_9CO_2]$ and $[C_2C_1Im][C_4F_9CO_2]$ [17]. On the other hand, $[C_4F_9SO_3]^-$ anion have lower α and higher β values, indicating a better packaging (Table 3).

The standard Gibbs free energy of aggregation, ΔG^0_{agg}, for the ionic surfactants [55] was also determined in this study, and the values reported in Table 3. The pseudophase model of micellization [55] was considered by determining the standard Gibbs free energy, ΔG^0_{agg}, for the ionic surfactants by Eq. 2:

$$\Delta G^0_{agg} = RT(1+\beta)\ln x_{CAC} \quad [2]$$

where R and T correspond to the universal gas constant and absolute temperature, respectively, and x_{CAC} is the critical aggregation concentration defined in terms of molar fraction. This parameter stands for the free energy accounted in transferring one mole of surfactant from the aqueous solution to the micellar pseudophase in the aggregates form [55]. When the parameter values are negative, a spontaneous aggregation of the surfactant molecules happens. Furthermore, all OH-FILs show an improved surfactant behaviour compared to the conventional surfactants, demonstrating the possibility to decrease the FILs toxicity and allowing biodegradability which is the key advantage to use OH-FILs in the biomedical field. All FILs, in all transitions, show that the aggregation behaviour is always spontaneous, with negative ΔG^0_{agg} values. More negative values were found for the non-functionalized FILs, especially for $[C_2C_1Im][C_4F_9SO_3]$, meaning an easy aggregation process for this IL.

Table 3

Critical aggregation concentrations, CACs, ionization degree, α, and Gibbs free energy of aggregation, ΔG^0_{agg}, of the fluorinated ionic liquids + water systems, determined by conductometry at 298.15 K.

		$[C_{2(OH)}C_1Im][C_4F_9SO_3]$	$[C_{2(OH)}C_1Im][C_4F_9CO_2]$	$[C_2C_1Im][C_4F_9SO_3]$[a]	$[C_2C_1Im][C_4F_9CO_2]$[b]
First CAC	x_{FIL}	0.0004	0.0003	0.0003	0.0004
	$mmol \cdot kg^{-1}$	19.65	18.32	14.55	20.96
	α	0.91	0.79	0.79	0.87
	ΔG^0_{agg} [$kJ \cdot mol^{-1}$]	-21.4	-24.1	-24.7	-22.1
Second CAC	x_{FIL}	0.0016	0.0012	0.0007	0.0014
	$mmol \cdot kg^{-1}$	87.98	63.19	38.54	77.23
	α	0.85	0.80	0.84	0.71
	ΔG^0_{agg} [$kJ \cdot mol^{-1}$]	-18.2	-20.1	-20.8	-20.9
Third CAC	x_{FIL}	0.0024	0.0022	0.0015	0.0070
	$mmol \cdot kg^{-1}$	125.8	119.0	81.03	341.4
	α	0.79	0.55	0.29	0.37
	ΔG^0_{agg} [$kJ \cdot mol^{-1}$]	-18.1	-21.9	-27.5	-20.0
Maximum	x_{FIL}	0.0509	0.0204	0.0867	–
	$mmol \cdot kg^{-1}$	1312	797	1667	–

Parameters from references (a) [16] and (b) [17].

4. Conclusions

The thermodynamic and thermophysical properties of hydroxyl functionalized FILs were determined in this work. Furthermore, the total miscibility and self-aggregation behaviour of OH-FILs + water systems were investigated. Results were compared with the analogous FILs, with the aim to evaluate the influence of adding a hydroxyl group to the structure of the imidazolium cation and how it affects FILs properties. The experimental study was completed with theoretical calculations of the density and viscosity of pure FILs and aqueous mixtures with the soft-SAFT EoS, using a set of transferable parameters in good agreement with the experimental data. This model will allow us to obtain other FILs properties that are not available experimentally.

Overall, the results show an increment in the density and viscosity of the pure OH-FILs and their aqueous mixtures with respect to the non-functionalized FILs, while a decrement of the thermal stability, melting temperature, free volume, ionicity and self-aggregation behaviour is noticed. However, when OH-FILs are compared with the conventional perfluorosurfactants, these novel compounds are total miscibility in the aqueous systems and show a higher surfactant behaviour. Furthermore, the lower ecotoxicity associated with the increment of the polarity by adding the hydroxyl group to FILs structure can be advantageous for the use of these compounds.

Acknowledgments

The authors would like to acknowledge C. Casas, M. Roy and C. Fialho, for their contribution in the experimental measurements.

Funding

Authors acknowledge financial support from FCT/MCTES (Portugal), through: grant SFRH/BD/130965/2017 (M.L.F.); Investigador FCT 2014 (IF/00190/2014 to A.B.P and IF/00210/2014 to J.M.M.A.); and projects PTDC/EQU-EQU/29737/2017, PTDC/QEQ-FTT/3289/2014 and IF/00210/2014/CP1244/CT0003. This work was also supported by Associate Laboratory for Green Chemistry–LAQV, financed by national funds from FCT/MCTES(UID/QUI/50006/2019). Additional funding has been provided by projects 2018-LC-01 and 2019-URL-IR1rQ-011, from Obra Social "La Caixa" and by Khalifa University through project RCII-2018-0024.

REFERENCES

[1] M. Deetlefs, M. Fanselow, K.R. Seddon, Ionic liquids: the view from Mount Improbable. RSC Adv., 6 (2016) 4280–4288. https://doi.org/10.1039/C5RA05829E

[2] K.S. Egorova, E.G. Gordeev, V.P. Ananikov, Biological activity of ionic liquids and their application in pharmaceutics and medicine. Chem. Rev., 117 (2017) 7132–7189. https://doi.org/10.1021/acs.chemrev.6b00562

[3] H. Ohno, M. Yoshizawa-Fujita, Y. Kohno, Functional design of ionic liquids: unprecedented liquids that contribute to energy technology, bioscience, and materials sciences. B. Chem. Soc. Jpn. 92 (2019) 852–868. https://doi.org/10.1246/bcsj.20180401

[4] N.S.M. Vieira, S. Stolte, J.M.M. Araújo, L.P.N. Rebelo, A.B. Pereiro, M. Markiewicz, Acute aquatic toxicity and biodegradability of fluorinated ionic liquids. ACS Sustain. Chem. Eng., 7 (2019) 3733–3741. https://doi.org/10.1021/acssuschemeng.8b03653

[5] S. Stolte, J. Arning, U. Bottin-Weber, A. Müller, W.-R. Pitner, U. Welz-Biermann, B. Jastorff, J. Ranke, Effects of different head groups and functionalised side chains on the cytotoxicity of ionic liquids. Green Chem., 9 (2007) 760–767. https://doi.org/10.1039/B615326G

[6] S. Stolte, M. Matzke, J. Arning, A. Böschen, W.-R. Pitner, U. Welz-Biermann, B. Jastorff, J. Ranke, Effects of different head groups and functionalised side chains on the aquatic toxicity of ionic liquids. Green Chem., 9 (2007) 1170–1179. https://doi.org/10.1039/B711119C

[7] D. Coleman, N. Gathergood, Biodegradation studies of ionic liquids. Chem. Soc. Rev., 39 (2010) 600–637. https://doi.org/10.1039/B817717C

[8] V.G. Krasovskiy, E.A. Chernikova, L.M. Glukhov, G.I. Kapustin, A.A. Koroteev, Effect of hydroxyl groups in a cation structure on the properties of ionic liquids. Russ. J. Phys. Chem. A, 92 (2018) 2379–2385. https://doi.org/10.1134/S003602441

[9] X.F. Liu, L.L. Dong, Y. Fang, Synthesis and self-aggregation of a hydroxyl-functionalized imidazolium-based ionic liquid surfactant in aqueous solution. J. Surfactants Deterg., 14 (2011) 203–210. https://doi.org/10.1007/s11743-010-1234-3

[10] S. Zhang, X. Qi, X. Ma, L. Lu, Y. Deng, Hydroxyl ionic liquids: the differentiating effect of hydroxyl on polarity due to ionic hydrogen bonds between hydroxyl and anions. J. Phys. Chem. B, 114 (2010) 3912–3920. https://doi.org/10.1021/jp911430t

[11] A.B. Pereiro, J.M.M. Araújo, S. Martinho, F. Alves, A. Matias, C.M.M. Duarte, L.P.N. Rebelo, I.M. Marrucho, Fluorinated ionic liquids: properties and applications, ACS Sustain. Chem. Eng. 1 (2013) 427-439. https://doi.org/10.1021/sc300163n

[12] N.S.M. Vieira, P.M. Reis, K. Shimizu, O.A. Cortes, I.M. Marrucho, J.M.M. Araújo, J.M.S.S. Esperança, J.N.C. Lopes, A.B. Pereiro, L.P.N. Rebelo, A thermophysical and structural characterization of ionic liquids with alkyl and perfluoroalkyl side chains. RSC Adv. 5 (2015) 65337–65350. https://doi.org/10.1039/C5RA13869H

[13] M.L. Ferreira, M.J. Pastoriza-Gallego, J.M.M. Araújo, J.N. Canongia Lopes, L.P.N. Rebelo, M.M. Piñeiro, K. Shimizu, A.B. Pereiro, Influence of nanosegregation on the phase behavior of fluorinated ionic liquids. J. Phys. Chem. C, 121 (2017) 5415–5427. https://doi.org/10.1021/acs.jpcc.7b00516

[14] R.E. Banks, B.E. Smart, J.C. Tatlow, Organofluorine chemistry – principles and commercial applications, Springer, US, New York, 1994. https://doi.org/10.1007/978-1-4899-1202-2

[15] M. Alves, N.S.M. Vieira, L.P.N. Rebelo, J.M.M. Araújo, A.B. Pereiro, M. Archer Fluorinated ionic liquids for protein drug delivery systems: Investigating their impact on the structure and function of lysozyme. Int. J. Pharmaceut., 526 (2017) 309−320. https://doi.org/10.1016/j.ijpharm.2017.05.002

[16] A.B. Pereiro, J.M.M. Araújo, F.S. Teixeira, I.M. Marrucho, M.M. Piñeiro and L.P.N. Rebelo, Aggregation behavior and total miscibility of fluorinated ionic liquids in water. Langmuir, 31 (2015) 1283–1295. https://doi.org/10.1021/la503961h

[17] N.S.M. Vieira, J.C. Bastos, C. Hermida-Merino, M.J. Pastoriza-Gallego, L.P.N. Rebelo, M.M. Piñeiro, J.M.M. Araújo, A.B. Pereiro, Aggregation and phase equilibria of fluorinated ionic liquids. J. Mol. Liq., 285 (2019) 386–396. https://doi.org/10.1016/j.molliq.2019.04.086

[18] N.S.M. Vieira, J.C. Bastos, L.P. Rebelo, A. Matias, J.M.M. Araújo, A.B. Pereiro, Human cytotoxicity and octanol/water partition coefficients of fluorinated ionic liquids. Chemosphere, 216 (2019) 576–586. https://doi.org/10.1016/j.chemosphere.2018.10.159

[19] F.J. Blas, L.F. Vega, Thermodynamic behaviour of homonuclear and heteronuclear lennard-jones chains with association sites from simulation and theory. Mol Phys. 92 (1997) 135–150. https://doi.org/10.1080/002689797170707

[20] M.L. Ferreira, J.M.M. Araújo, A.B. Pereiro, L.F. Vega, Insights into the influence of the molecular structure of Fluorinated Ionic Liquids on their thermophysical properties. A soft-SAFT

based approach. Phys. Chem. Chem. Phys. 21 (2019) 6362–6380. https://doi.org/10.1039/C8CP07522K

[21] F.J. Blas, L.F. Vega, Prediction of binary and ternary diagrams using the statistical associating fluid theory (SAFT) equation of state. Ind. Eng. Chem. Res. 37 (1998) 660–674. https://doi.org/10.1021/ie970449+

[22] W.G. Chapman, K.E. Gubbins, G. Jackson, M. Radosz, SAFT: equation-of-state solution model for associating fluids. Fluid Phase Equilib. 52 (1989) 31–38. https://doi.org/10.1016/0378-3812(89)80308-5

[23] W.G. Chapman, K.E. Gubbins, G. Jackson, M. Radosz, New reference equation of state for associating liquids. Ind. Eng. Chem. Res. 29 (1990) 1709–1721. https://doi.org/10.1021/ie00104a021

[24] M.S. Wertheim, Fluids with highly directional attractive forces: I. Statistical thermodynamics, J. Stat. Phys. 35 (1984) 19–34. https://doi.org/10.1007/BF01017362

[25] M.S. Wertheim, Fluids with highly directional attractive forces: II. Thermodynamic-perturbation theory and integral-equations, J. Stat. Phys. 35 (1984) 35–47. https://doi.org/10.1007/BF01017363

[26] M.S. Wertheim, Fluids with highly directional attractive forces: III. Multiple attraction sites, J. Stat. Phys. 42 (1984) 459–476. https://doi.org/10.1007/BF01127721

[27] M.S. Wertheim, Fluids with highly directional attractive forces: IV. Equilibrium polymerization, J. Stat. Phys. 42 (1986) 477–492. https://doi.org/10.1007/BF01127722

[28] A.B. Pereiro, F. Llovell, J.M.M. Araújo, A.S. Santos, L.P.N. Rebelo, M.M. Piñeiro, L.F. Vega, Thermophysical characterization of ionic liquids based on the perfluorobutanesulfonate anion: experimental and soft-SAFT modelling results. ChemPhysChem. 18 (2017) 2012–2023. https://doi.org/10.1002/cphc.201700327

[29] M.L. Ferreira, F. Llovell, L.F. Vega, A.B. Pereiro, J.M.M. Araújo, Systematic study of the influence of the molecular structure of fluorinated ionic liquids on the solubilization of atmospheric gases using a soft-SAFT based approach. J. Mol. Liq. (2019) 111645. https://doi.org/10.1016/j.molliq.2019.111645

[30] F. Llovell, E. Valente, O. Vilaseca, L.F. Vega, Modeling complex associating mixtures with [C_n-mim][Tf_2N] ionic liquids: Predictions from the soft-SAFT equation. J. Phys. Chem. B 115 (2011) 4387–4398. https://doi.org/10.1021/jp112315b

[31] M.B. Oliveira, F. Llovell, J.A.P. Coutinho, L.F. Vega, Modeling the [NTf_2] pyridinium ionic liquids family and their mixtures with the soft statistical associating fluid theory equation of state. J. Phys. Chem. B 116 (2012) 9089–9100. https://doi.org/10.1021/jp303166f

[32] F. Llovell, L.F. Vega, Assessing ionic liquids experimental data using molecular modeling: [$C_n$mim][BF_4] case study. J. Chem. Eng. Data 59 (2014) 3220–3231. https://doi.org/10.1021/je5002472

[33] M.B. Oliveira, E.A. Crespo, F. Llovell, L.F. Vega, J.A.P. Coutinho, Modeling the vapor–liquid equilibria and water activity coefficients of alternative refrigerant-absorbent ionic liquid–water pairs for absorption systems. Fluid Phase Equilib. 426 (2016) 100–109. https://doi.org/10.1016/j.fluid.2016.02.017

[34] S.R. Urahata, M.C.C.J. Ribeiro, Structure of ionic liquids of 1-alkyl-3-methylimidazolium cations: A systematic computer simulation study. J. Chem. Phys. 120 (2004) 1855–1863. https://doi.org/10.1063/1.1635356

[35] T.I. Morrow, E.J. Maginn, Molecular dynamics study of the ionic liquid 1-N-butyl-3-methylimidazolium hexafluorophosphate. J. Chem. Phys. B 106 (2002) 12807–12813. https://doi.org/10.1021/jp0267003

[36] M.G. Del Pópolo, G.A. Voth, On the structure and dynamics of ionic liquids. J. Phys. Chem. B 108 (2004) 1744–1752. https://doi.org/10.1021/jp0364699

[37] T.A. Halgren, MMFF VII. Characterization of MMFF94, MMFF94s, and other widely available force fields for conformational energies and for intermolecular-interaction energies and geometries. J. Comput. Chem. 20 (1999) 730–748. https://doi.org/10.1002/(SICI)1096-987X(199905)20:7<730:AID-JCC8>3.0.CO;2-T

[38] M.D. Hanwell, D.E. Curtis, D.C. Lonie, T. Vandermeersch, E. Zurek, G.R. Hutchison, Avogadro: an advanced semantic chemical editor, visualization, and analysis platform. J. Cheminformatics, 4 (2012) 17. https://doi.org/10.1186/1758-2946-4-17

[39] Pàmies Corominas, J. Bulk and interfacial properties of chain fluids: a molecular modelling approach. Tarragona, Spain: Universitat Rovira i Virgili; 2004. ISBN: 8468874280.

[40] L.F. Vega, F. Llovell, F.J. Blas, Capturing the solubility minima of n-alkanes in water by soft-SAFT. J Phys. Chem. B. 113 (2009) 7621–7630. https://doi.org/10.1021/jp9018876

[41] S. Zhang, N. Sun, X. He, X. Lu, X. Zhang, Physical properties of ionic liquids: database and evaluation. J. Phys. Chem. Ref. Data, 35 (2006) 1475–1517. https://doi.org/10.1063/1.2204959

[42] S. Aparicio, M. Atilhan, F. Karadas, Thermophysical properties of pure ionic liquids: review of present situation. Ind. Eng. Chem. Res. 2010, 49, 9580–9595. https://doi.org/10.1021/ie101441s

[43] M. Tariq, P.A.S. Forte, M.F.C. Gomes, J.N.C. Lopes, L.P.N. Rebelo, Densities and refractive indices of imidazolium-and phosphonium-based ionic liquids: Effect of temperature, alkyl chain length, and anion. J. Chem. Thermodyn., 41 (2009) 790–798. https://doi.org/10.1016/j.jct.2009.01.012

[44] N.S.M. Vieira, A. Luís, P.M. Reis, P.J. Carvalho, J.A. Lopes-da-Silva, J.M.S.S. Esperança, J.M.M. Araújo, L.P.N. Rebelo, M.G. Freire, A.B. Pereiro, Fluorination effects on the thermodynamic, thermophysical and surface properties of ionic liquids. J. Chem. Thermodyn. 97 (2016) 354–361. https://doi.org/10.1016/j.jct.2016.02.013

[45] F. Llovell, R.M. Marcos, L.F. Vega, Free-volume theory coupled with soft-SAFT for viscosity calculations: comparison with molecular simulation and experimental data. J. Phys. Chem. B 117 (2013) 8159–8171. https://doi.org/10.1021/jp401307t

[46] F. Llovell, R.M. Marcos, L.F. Vega, Transport properties of mixtures by the soft-SAFT + Free-volume theory: application to mixtures of n -alkanes and hydrofluorocarbons. J. Phys. Chem. B 117 (2013) 5195–5205. https://doi.org/10.1021/jp401754r

[47] M.R. Moldover, IUPAC Experimental Thermodynamics Vol. VI: Measurement Thermodynamic Properties of Single Phases, Elsevier, (2008) 435-451. ISBN: 9780080531441

[48] E. Cané, F. Llovell, L.F. Vega, Accurate viscosity predictions of linear polymers from n-alkanes data. J. Mol. Liq. 243 (2017) 115–123. https://doi.org/10.1016/j.molliq.2017.08.033

[49] F. Llovell, O. Vilaseca, N. Jung, L.F. Vega, Water+1-alkanol systems: modeling the phase, interface and viscosity properties. Fluid Phase Equilib. 360 (2013) 367–378. https://doi.org/10.1016/j.fluid.2013.10.002

[50] J.N. Phillips, The energetics of micelle formation. Trans. Faraday. Soc. 51 (1955) 561−569. https://doi.org/10.1039/TF9555100561

[51] F.S. Teixeira, N.S.M. Vieira, O.A. Cortes, J.M.M. Araújo, I.M. Marrucho, L.P.N. Rebelo, A.B. Pereiro, Phase equilibria and surfactant behavior of fluorinated ionic liquids with water. J. Chem. Thermodyn., 82 (2015) 99−107. https://doi.org/10.1016/j.jct.2014.10.021

[52] E. Szajdzinska-Pietek, M. Wolszczak, Time-resolved fluorescence quenching study of aqueous solutions of perfluorinated surfactants with the use of protiated luminophore and quencher, Langmuir, 16 (2000) 1675−1680. https://doi.org/10.1021/la990981x

[53] A. González-Pérez, J.M. Ruso, G. Prieto, F. Sarmiento, Apparent molar quantities of sodium octanoate in aqueous solutions, Colloid Polym. Sci. 282 (2004) 1133−1139. https://doi.org/10.1007/s00396-003-1047-2

[54] J.L. López-Fontán, F. Sarmiento, P.C. Schulz, The aggregation of sodium perfluorooctanoate in water, Colloid Polym. Sci. 283 (2004) 862−871. https://doi.org/10.1007/s00396-004-1228-7

[55] R. Zana, Critical micellization concentration of surfactants in aqueous solution and free energy of micellization. Langmuir 12 (1996) 1208−1211. https://doi.org/10.1021/la950691q